

Numerical modelling of airflow over an idealised transverse dune

Daniel R. Parsons ^{a,* 1}, Giles F.S. Wiggs ^a, Ian J. Walker ^b, Robert I. Ferguson ^a,
Brian G. Garvey ^a

^a *Department of Geography, University of Sheffield, Winter Street, Sheffield, S10 2TN, UK*

^b *Department of Geography, University of Victoria, P.O. Box 3050, Victoria, British Columbia, V8W 3P5, Canada*

Received 12 August 2002; received in revised form 10 January 2003; accepted 18 February 2003

Abstract

The general flow structure over transverse aeolian dunes is now well documented through both field studies and wind tunnel experiments. Research on windward (stoss) slopes of dunes is extensive and has recently been complemented by research on the lee-side flow structure. However, a number of technical deficiencies in wind tunnel instrumentation and a lack of detailed resolution in and appropriate turbulence instrumentation for field research have resulted in an incomplete quantified characterisation of the flow structure over aeolian dunes. This study applies a two-dimensional numerical model with an RNG-modified κ - ϵ turbulence model to simulate the time-averaged flow field over an idealized aeolian dune. The model is successfully validated with wind tunnel experimental data. Results indicate that the model accurately predicts the flow patterns over the dune, producing regions of flow stagnation at the toe, acceleration up the stoss slope and a region of flow separation and reversal in the lee. Further development and application of this model will allow examination of flow-form interaction, the testing of more complex isolated dune morphologies, and characterisation of flow over multiple dunes.

© 2003 Elsevier Ltd. All rights reserved.

Keywords: Aeolian dunes; Airflow; Numerical modelling; Computational fluid dynamics (CFD); Aeolian processes

Software availability

This paper applies Parabolic Hyperbolic Or Elliptic Numerical Integration Code Series (PHEONICS) supplied by Concentration Heat & Momentum Ltd., Bakery House, 40 High Street, Wimbledon Village, London, SW19 5AU, UK. Tel: +44 (208) 947 7651 ; Fax: +44 (208) 879 3497.

1. Introduction

There has been much recent interest in the complex interactions between sand dune morphology, windflow and sediment transport (McKenna Neuman et al., 1997, 2000; Wiggs, 2001; Walker and Nickling, 2002a). Research concerning secondary flow regimes governing dune-flow interactions and the existence of a dynamic

equilibrium between dune morphology and windflow patterns has dominated recent dune literature (see reviews by Nickling and McKenna Neuman, 1999; Wiggs, 2001). The research focus on the dynamics of dune windward slopes (e.g., Lancaster et al., 1996; Frank and Kocurek, 1996a; Wiggs et al., 1996; McKenna Neuman et al., 2000) has been complemented by similar field and wind tunnel studies investigating flow patterns and sediment dynamics in the turbulent lee-side eddies downwind of transverse dune crests (Frank and Kocurek, 1996b; Walker and Nickling, 2002a). The acceleration of windspeed and surface shear stress to a maximum on the stoss slopes of sand dunes followed by lee-side flow separation and a region of flow recovery are now well documented. Progress is still hampered, however, by the small number of field sites investigated and by the limited dune geometries that have been experimented upon in wind tunnel studies. In addition, due to instrument design limitations, regions of highly turbulent or reversed flow have not been quantified in wind tunnel experiments. For example, Walker and Nickling (2002b) had to omit the velocity measurements in the lee side

* Corresponding author.

E-mail address: parsons@earth.leeds.ac.uk (D.R. Parsons).

¹ Present address: School of Earth Sciences, University of Leeds, Woodhouse Lane, Leeds, LS2 9JT, UK.

reverse eddy. This has resulted in a lack of quantification, and thus deficient understanding, of the flow structure in the dune lee.

Whilst physical experimentation has provided us with a substantial insight into a number of flow-form interactions (e.g., flow acceleration, crestal separation, re-circulation, re-attachment, flow recovery, etc.), questions remain as to the sensitivity, structure, and dynamic function of these interactions with changing dune geometry. An adaptable and rapid method by which our understanding of flow patterns can be further improved involves numerical modelling of the flow field over different dune geometries. Previous attempts to model the turbulent boundary layer over isolated dunes (e.g., Howard et al., 1977; Wippermann and Gross, 1986; Stam, 1997) have been hampered by the lack of detailed empirical data against which the models could be validated. Furthermore, the models used to calculate flow structure over dune forms often have had severe limitations. For example, Stam (1997) applied an analytical flow model based on a boundary-layer model (e.g., Jackson and Hunt, 1975), which is unable to solve the reversed flow in lee-side eddies often present over dune forms. This limits the calculation of flow structures to low angle dunes where lee-side eddies are not present. Stam (1997) noted that numerical techniques are required to successfully simulate flows over a greater range of dune forms.

With the recent proliferation of field and wind tunnel data concerning dune processes it is now appropriate to apply new refinements in numerical calculations of flow fields over bedforms using computational fluid dynamics (CFD) to provide new insight into dune flow dynamics and related sand transport mechanisms.

This paper represents the first stage in applying a numerical CFD code (PHOENICS™ 3.4) to generate flow field patterns over dunes and validates the simulated flow field against wind tunnel derived experimental data (from Walker and Nickling, 2002b). This validation will serve as the basis for further examination of the variation in the flow field around both isolated and closely-spaced dunes of differing geometries in forthcoming papers.

2. Computational fluid dynamics (CFD)

In the last few years, there has been a proliferation of the use of two and three-dimensional CFD in fluvial geomorphology and hydrology (see Bates and Lane, 1998). These models enable an improved simulation of important fluid processes thereby providing prediction fields that enhance insight into the spatial distribution and sedimentological significance of these processes. CFD modelling offers a new methodology that is complementary to traditional field and laboratory approaches. These models provide details of the flow field that are

often difficult to measure and offer controlled conditions in which certain aspects of the experimental set up can be varied rapidly. For example, Hodkinson and Ferguson (1998) applied a three-dimensional numerical model to investigate and identify the controls on flow separation at the concave bank of river meander bends. Bradbrook et al. (1998) applied a similar model to ascertain the controls on secondary circulation in simple river confluence geometries. Numerical flow modelling has also been applied to investigate flow fields over sub-aqueous sand dunes (Yoon and Patel, 1996) with reasonable validation to experimental flume data.

3. The numerical model

3.1. Background and solution details

This paper employs the code PHOENICS™ 3.4, which is one of several commercially available CFD programs. The model used in this study solves the elliptic form of the Reynolds-averaged Navier–Stokes equations in two dimensions with a finite volume method (see Versteeg and Malalasekera, 1995). In CFD simulations, scalar values are stored at the cell centres, but vector values are stored at the centres of the cell faces, necessitating the use of interpolation assumptions. The interpolation scheme applied to simulations in this paper is hybrid-upwind, where central differences between cells are used for the calculations where diffusion dominates and upwind differences are used where convection is high, with the Peclet filter set equal to 2. The hybrid-upwind scheme is only first order accurate and can suffer from numerical diffusion when flow is highly skewed relative to the grid. Nevertheless, it is more stable than higher order schemes and investigations analogous to this present one have indicated that errors due to the interpolation scheme are not likely to be significant (Waterson, 1994).

The pressure and momentum equations are coupled through the SIMPLEST algorithm [a variation of SIMPLE (Pantaankar and Spalding, 1972)] where pressure and velocity fields are iteratively calculated until continuity errors in mass and momentum are adequately small. In this study, numerical convergence required that mass and momentum flux residuals reduced to 0.01% of the inlet flux and that pressure values at a reference point above the dune crest were changing by less than 0.1% per iteration.

Owing to current computational limits, the simulation of all turbulent motions in a complex flow field is infeasible. This is due to the necessity of all grid cells in the domain being smaller than the smallest turbulent motion and that time steps in an unsteady calculation are smaller than the fastest turbulent motion. Therefore, Reynolds averaging is applied where variables are split into a mean

Table 1
Constants for both the standard and the RNG modified κ - ϵ turbulence models

	C_μ	$C_{\epsilon 1}$	$C_{\epsilon 2}$	σ_κ	σ_ϵ
Standard κ - ϵ	0.090	1.44	1.92	1.00	1.30
RNG modified	0.084	1.42	1.68	0.72	0.72

value and a superimposed random variation. This introduces a number of new terms (the Reynolds shear stresses) into the Navier–Stokes equations. To calculate these stresses the use of semi-empirical turbulence models is required. These models thus represent the effect of turbulent momentum transfer on the mean flow field, producing a time-averaged solution in which turbulent effects are accounted for. In this study, the two-equation κ - ϵ model, modified by renormalization group theory (Yakhot et al., 1992), is applied. This turbulence model has modified constants from the standard two-equation κ - ϵ model (Table 1) and is recommended for simulating flows with significant mean strain and shear. For example, it has been shown to perform better in the prediction of sheared and re-circulating flows over backward facing steps (e.g., Bradbrook et al., 1998).

3.2. Boundary conditions

Mass flux values must be specified for each grid cell in the upstream inflow, providing an incoming velocity profile for the model. In order to simulate upwind effects of the dune (e.g., pressure stagnation and flow deceleration), a profile had to be specified far enough upstream of the dune. However, the laboratory experiment had been carried out for its own purposes and a comparable velocity profile was not available far enough upstream of the dune (Fig. 1). In order to solve this problem a series of plane-bed model runs were conducted to determine an incoming velocity profile that produced a profile that closely matched the measured plane-bed profile at the point of dune intersection (Fig. 2). This calculated incoming profile was then used in all model runs with the dune inserted.

At the outlet profile, the pressure is fixed at zero for all cells and calculated pressure values in the domain are

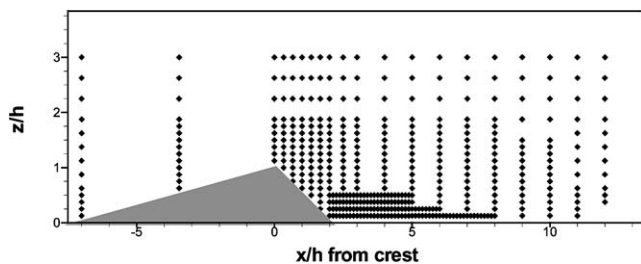


Fig. 1. Dune form and the positions of validation points.

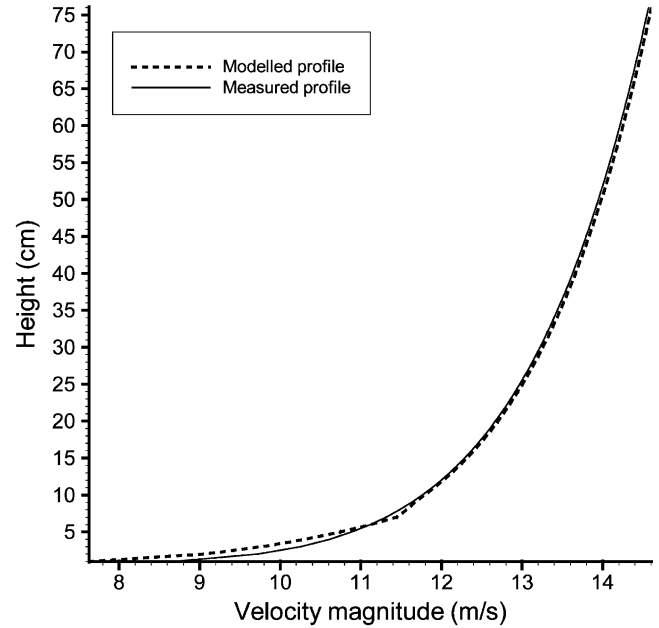


Fig. 2. Comparison of modelled and measured incoming windspeed profiles in plane bed profiles at the location of the dune toe.

defined relative to this. Consequently, the outlet had to be far enough away from the effects of the negative pressure zone in the dune lee to stop inflow at the outlet.

In the cell at the fluid–solid interface, it was necessary to prescribe conditions for the velocity and turbulence parameters. For this purpose, the universal ‘Law of the Wall’ (1) was applied in the bottom cell in the domain.

$$\frac{u_p}{u_\tau} = \frac{\ln(EZ^+)}{\kappa} \quad (1)$$

$$u_\tau = \sqrt{\tau/\rho} \quad (2)$$

$$Z^+ = u_\tau Z/\mu \quad (3)$$

where u_τ is the shear velocity, Z^+ is the non-dimensional wall node distance, κ is the von Karman constant (0.4), u_p is velocity parallel to the wall, τ is bed shear stress, ρ is fluid density, Z is the normal distance to the wall, μ is the laminar viscosity, and E is the roughness parameter which in all models was set equal to 9.0 for the case of a smooth boundary.

The form of the dune had to be represented within the model and this could be done in one of two main ways: boundary fitted co-ordinates or a porosity treatment. In CFD modelling objects are traditionally represented by boundary fitted co-ordinates, where the computational grid is deformed around objects and they are thus outside the computed domain. This poses major problems for the representation of a dune-like form, as the grid has to be highly deformed and horizontal gridlines at the crest of the dune meet at high angles causing large amounts of numerical diffusion and problems obtaining a converged solution. The dune can also be represented

in a Cartesian grid through the application of porosity type treatments where cells are within the solution domain but are blocked out to stop flow through them. For instance, if the centre of a cell falls inside a solid, the entire cell is taken to be solid while if it falls in the fluid, the entire cell is open to flow. This approach poses difficulties as sloping or curved surfaces are represented in a ‘stair-case’ fashion. To resolve this issue, finer grid volumes can be used to increase the grid density near a surface, and thus improve the resolution. Nevertheless, such a representation is often inadequate and results in unacceptable loss of pressure and produces spurious predictions close to the boundary. However, recent developments (Spalding and Zhang, 1996; Yang et al., 1997a,b) provide an alternative to the ‘stair-case’ method called the ‘cut-cell’ technique where intersections of the geometry with the grid lines are determined and the areas and volumes of partially blocked cells are calculated. The equation formulation is then modified to account for the local non-orthogonal intersection, resulting in significantly enhanced predictions. This ensures a higher degree of precision in representing the true geometry of the boundary of contact between the fluid and solid and thereby increases the accuracy of simulated near-surface flow dynamics. The ‘cut-cell’ approach was applied in all simulations in this study.

4. Model validation and verification

4.1. Model validation

In order to ascertain the capabilities of the model it was initially used to predict the measured flow velocities for the wind tunnel experiment of Walker and Nickling (2002b). The experiment was conducted in the sediment transport wind tunnel in the Department of Geography, University of Guelph. The wind tunnel was of re-circulating design and was 8.0 m long by 0.92 m wide by 0.76 m high. A smooth plywood dune, based on a simplified two-dimensional profile of a field dune (at 1:18 scale) investigated by Walker (1999), was constructed and placed in the tunnel 7.0 m from the leading edge of the tunnel (Table 2). The model occupied the full width of

Table 2
Dune experimental details

Dimension	Measurement
Dune height	0.08 m
Total base length	0.72 m
Lee base length	0.16 m
Stoss base length	0.56 m
Aspect ratio	0.143
Lee slope angle	27.0°
Stoss slope angle	7.6°

the working section and was orientated with the crestline transverse to the flow direction.

A constant freestream velocity (u_∞) of 13 m s^{-1} was maintained and was measured at 0.4 m (5 h) above the bed and downwind of the dune, using a pitot tube and digitally monitored pressure transducer. Point measurements were taken using a TSI® IFA 300 constant temperature hot-film anemometer (cross-probe) system. The probe was attached to a TSI-engineered 90° elbow on a probe extension that entered the working section through a self-sealing groove cut into the dune model. All points sampled were approximately 7 m from the inlet bell to ensure fully developed boundary layer conditions. A total of 735 points were sampled in twenty vertical profiles spanning 0.9 m of the tunnel and reaching a maximum height of 0.25 m, with additional measurements taken in a 0.5 cm grid in the lee of the dune (Fig. 1). Measurements were sampled at a frequency of 100 Hz for 10.24 s and yielded instantaneous horizontal (U) and vertical (V) velocities, Reynolds stress (RS), streamline angle (ϕ) and turbulent moment statistics. The directional response limits of this type of probe are $\pm 30^\circ$ and readings are also dubious at turbulence intensity values above 40% (Mertati and Adrian, 1984; Wright, 1998), meaning that the probe was unable to resolve regions of reversed flow.

To enhance characterization of flow in the separation cell, flow visualization was employed over the model using an array of streamer masts. Masts were inserted into the wind tunnel model from above with nylon thread attached at regular intervals, permitting investigation of the qualitative flow pattern, the extent of the lee separation cell, and the point of reattachment (Fig. 3).

A CFD model was constructed which matched the dimensions of the wind tunnel experiment. Model validation was based on 415 predicted points within the model domain, which coincided with the locations of measurements taken in the wind tunnel (Fig. 1). The downstream velocity component shows good agreement between modelled and measured values with a high correlation coefficient ($r = 0.98$) and the 1:1 line in close agreement, particularly for higher velocity values (Table 3; Fig. 4a). However, there is a significant zone of disagreement for the lower velocities such that predicted velocities are negative whilst measured values are positive. These points are from the lee separation zone where, due to design limitations, the wind tunnel measuring probe was unable to resolve the highly turbulent and negative velocities. Qualitative comparison of the flow patterns indicated by visualization streamers (Fig. 3) and the predictions from the numerical model (Fig. 5a) reveal that the numerical model is correctly simulating the reverse velocities that are clearly present in this region.

Although slightly weaker, the agreement between measured and predicted values of vertical velocity

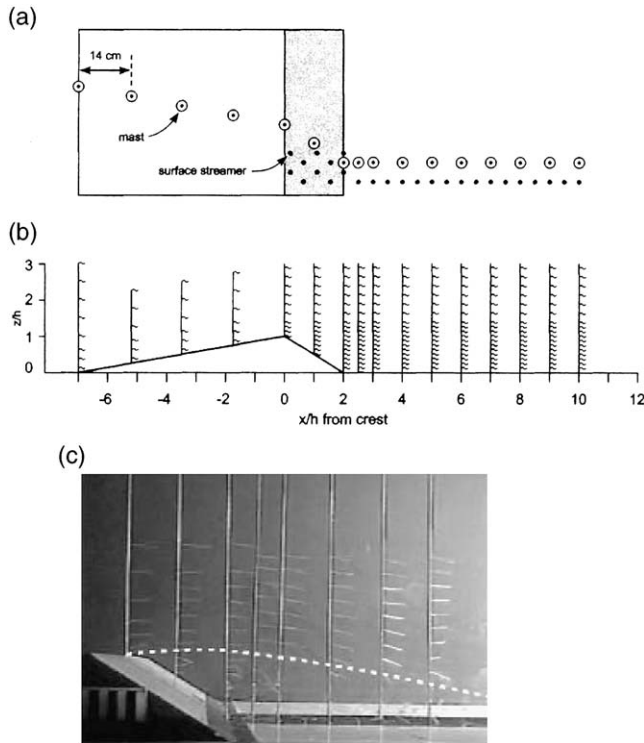


Fig. 3. Flow streamer deployment used for flow visualization in the wind tunnel study of Walker and Nickling (2002b).

(Table 3; Fig. 4b) is still relatively high ($r = 0.83$), especially as the range of values is low and most points are clustered close to the origin. Although agreement is generally good there is considerable disagreement in three distinct areas: (1) a vertical line of points where the model predicts very high positive values in comparison with the slightly negative measured values; (2) a group of points in the bottom left of the graph where the measured values are more negative than the predicted and; (3) a small group of points extending toward the top right between the line of best fit and the 1:1 line. The first group of points is explained by the high positive vertical velocities that are predicted by the model flowing up the lee of the dune in the separation zone but are not correctly measured by the probe (Fig. 5b). The second area are points within the flow re-attachment region, where the model predicts lower velocities overall, perhaps due to energy dissipation through high turbu-

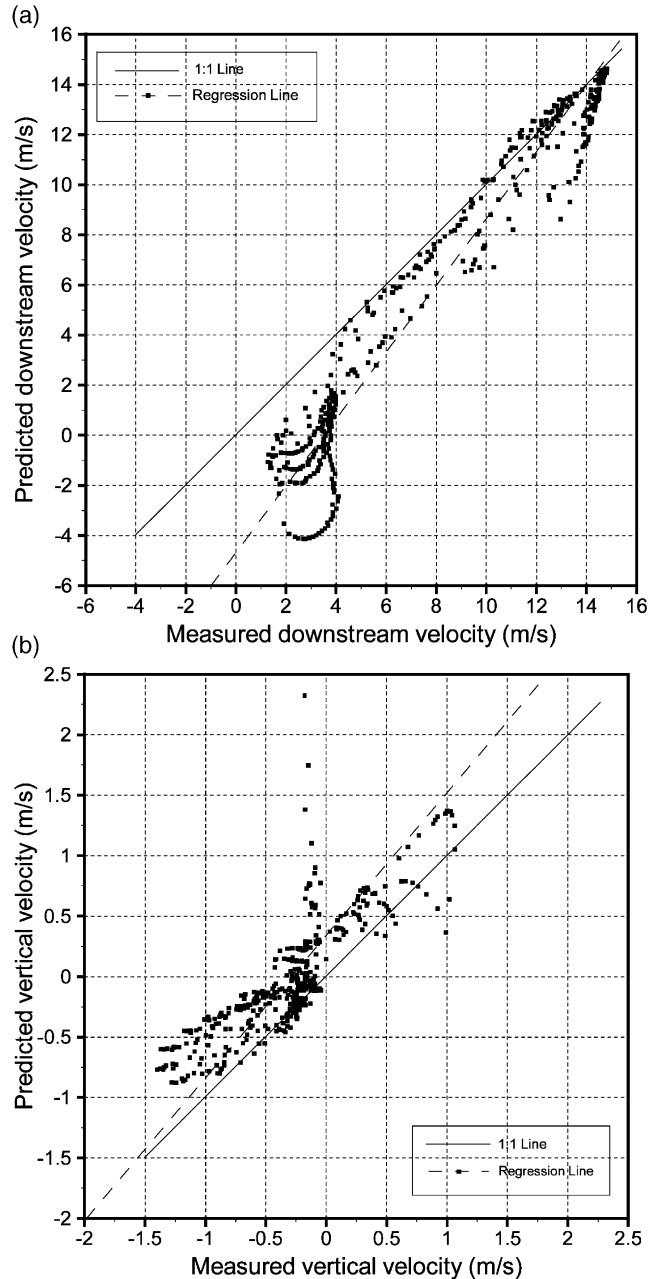


Fig. 4. Comparison of modelled to measured velocities (a) stream-wise (U) and (b) vertical (V).

Table 3

Linear regression results between predicted and measured variables for all validation points ($n = 415$) and for all points excluding those within the dune lee separation zone (212)

Variable	b Coefficient	Correlation Coefficient
Streamwise velocity (all points)	1.41	0.98
Vertical velocity (all points)	1.03	0.83
Streamwise velocity (excluding separation zone)	1.29	0.95
Vertical velocity (excluding separation zone)	1.03	0.88

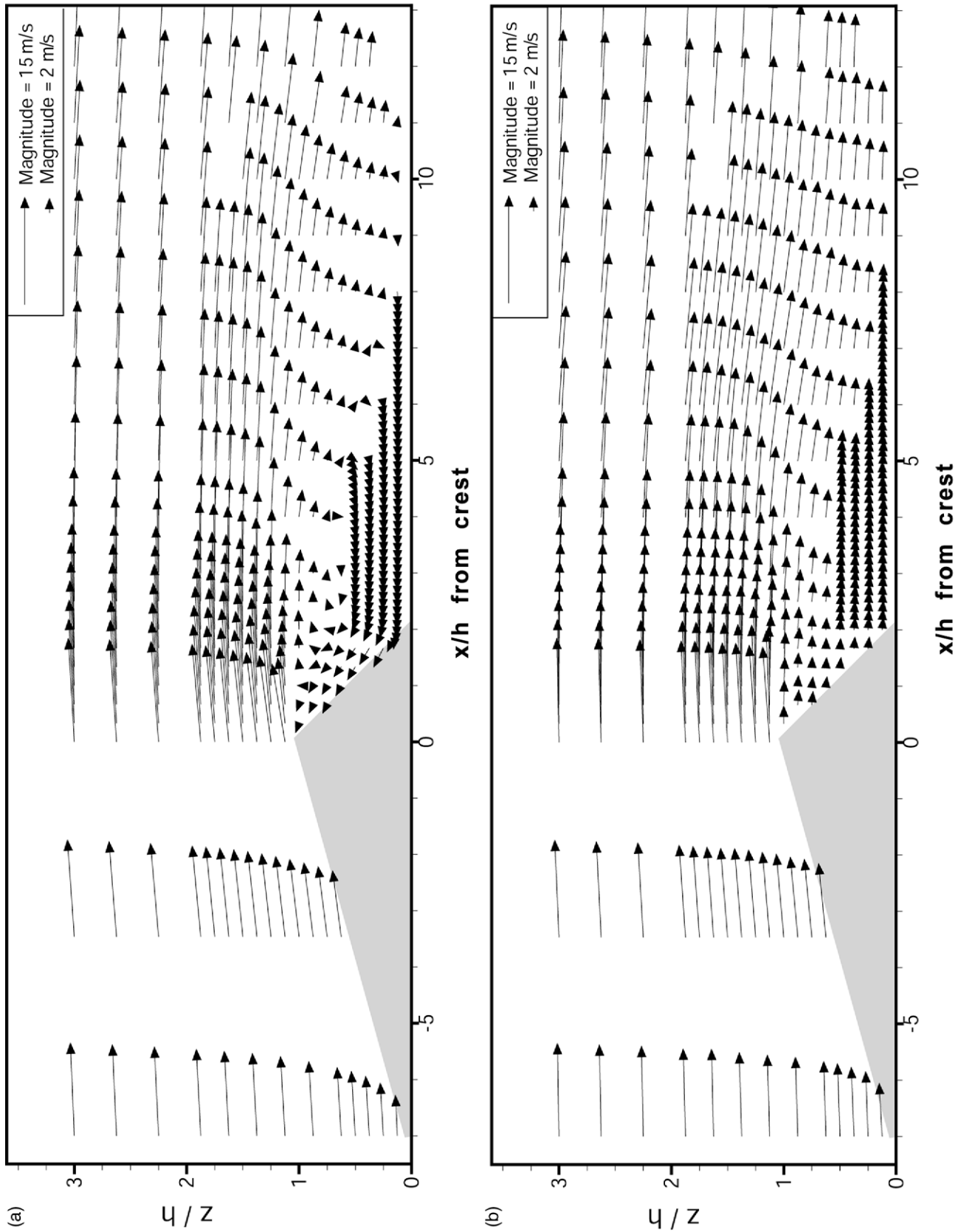


Fig. 5. Flow vectors over the dune (a) modelled and (b) experimental (measured in the wind tunnel study of Walker and Nickling (2002b)).

lence intensities that would again compromise the measurement probe’s performance. Finally, the third area of disagreement is due to the model slightly over predicting the stoss side vertical velocity components (Fig. 5), perhaps due to the small differences in the incoming velocity profile between the wind tunnel and the numerical model (Fig. 2).

Although there are some notable differences between the measured and modelled results, they are primarily due to the limitations of the measuring instrument rather than that of the numerical model. In regions where the instrument is known to perform well the match is very good. Indeed removal of the validation points in the lee re-circulation zone improves the relationships (Table 3), with a considerable increase in the vertical velocity correlation and although there is slight decline in the streamwise velocity correlation, there is a significant movement of the regression line towards that of equality. Furthermore, qualitative assessment of the predicted flow patterns and the indications given by the streamers (Fig. 3) confirm the presence and extent of the separation zone, which is successfully simulated by the numerical model. It is therefore suggested that the performance of the numerical model is satisfactory for both the investigation of the mean flow structures over the dune, particularly in the lee, and for future experiments where different aspects of dune form and spacing can be investigated.

4.2. Model verification

The main variable investigated for verification is the sensitivity of the solution to the grid resolution. As grid resolution increases the accuracy of the solution is increased although computational time is also significantly increased. Simulations using four different uniform grid resolutions were run (Table 4). The results of the grid sensitivity analysis indicated that there was little difference between grid resolutions of 0.5–2 cm, but that the accuracy of the solution was reduced in the coarsest grid resolution of 4 cm (Fig. 6). Thus for computational reasons, including significantly reduced computing time and impact on the feasibility of conducting numerous

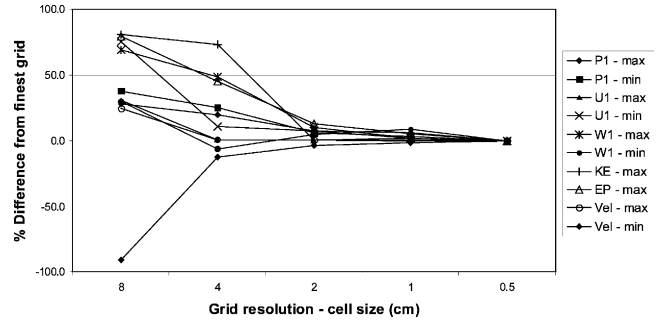


Fig. 6. Effect of varying grid resolution on key flow predictions.

other simulations for future experiments, a grid resolution of 2 cm was chosen for the validation to experimental data. This is the coarsest grid resolution possible without any significant reductions in model accuracy.

5. Discussion

The model run used for validation against the experimental wind tunnel data was examined to ascertain the predicted flow structure around the dune. Figs. 7–10 show the pressure ($N\ m^{-2}$), streamwise velocity (U , $m\ s^{-1}$), vertical velocity (V , $m\ s^{-1}$), and turbulent kinetic energy (TKE, $m^2\ s^{-2}$) fields around the dune as predicted by the model.

Figs. 7 and 8 show that the pressure and streamwise velocity predicted by the model conform to the expected pressure gradients over dunes identified in previous research (see Wiggs, 2001; Walker and Nickling,

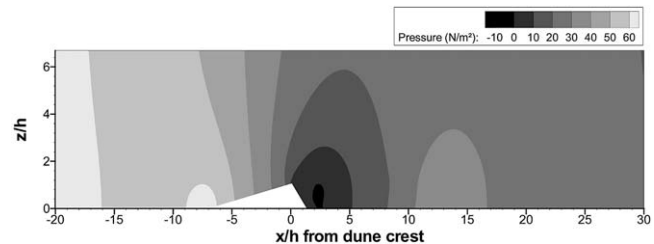


Fig. 7. Modelled pressure field over an idealized, isolated transverse dune.

Table 4
Dimensions of the four uniformly spaced grid resolutions used in model verification

Grid number	Number of cells in each direction			Individual grid cell size (m)
	X	Y	Z	
Grid 1	1960	1	152	0.005
Grid 2	980	1	76	0.010
Grid 3	490	1	38	0.020
Grid 4	245	1	19	0.040
Grid 5	123	1	10	~0.080

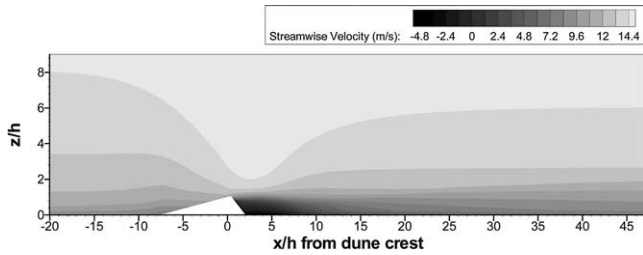


Fig. 8. Modelled streamwise velocity (U) field over an idealized, isolated transverse dune.

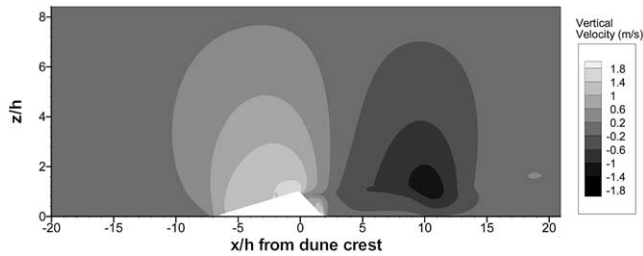


Fig. 9. Modelled vertical velocity (V) field over an idealized, isolated transverse dune.

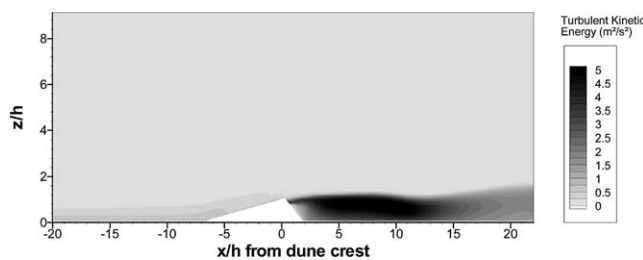


Fig. 10. Modelled turbulent kinetic energy (TKE) field over an idealized, isolated transverse dune.

2002a). Upwind of and at the toe of the windward slope velocity is retarded due to an adverse (increasing) pressure gradient as the flow approaches the dune body. This zone of increasing pressure extends approximately two dune heights both upwind and downwind of the toe itself and results in a near-surface velocity reduction of about 20%. The magnitude and spatial extent of this velocity reduction is consistent with published field data of windflow over dunes (Wiggs et al., 1996; McKenna Neuman et al., 1997). The geomorphological significance of this low velocity zone at the toe of dunes has been highlighted by Wiggs (1993); Wiggs et al. (1996) and Walker and Nickling (2002a). Assuming a positive relationship between mean wind velocity and the capacity of the wind to transport sediment, this region of low wind velocity should become a zone of deposition in high-energy wind conditions when sand is transported by the approach flow. Deposition is rarely observed here in the field. Wiggs et al. (1996) explain the maintenance of sediment transport through this region as a consequence of concave streamline curvature resulting in increased

turbulence intensity and Reynolds stresses. This argument requires the onset of streamline curvature to coincide with the upwind edge of the adverse pressure gradient. Vertical flow velocities predicted by the model and shown in Fig. 9 suggest that there is no upward movement in the mean streamlines upwind of the dune toe. Such a result is in contrast to wind tunnel measurements of streamline angles and vertical velocities presented by Wiggs et al. (1996). The absence of prediction by the model of concave curvature of streamlines in the toe region may be due to the relatively low angle (8°) of, and lack of concavity or convexity in, the windward slope of the model. Future model runs will investigate the effects of more complex (and realistic) windward slope morphologies to investigate this point further.

Nevertheless, there is evidence to support the idea of increased turbulence intensity in the toe region of the dune. Fig. 10 shows predicted turbulent kinetic energy (TKE) over the model dune. TKE is the sum of predicted sum of mean squares of the horizontal (U') and vertical (V') fluctuating components of the wind flow. The value of TKE in the toe region of the dune is stable whilst the mean horizontal windflow (U) is predicted to reduce in this region (Fig. 8). The relative importance of the fluctuating component of the windflow (TKE) must therefore increase in this low velocity region. Such an increase in the relative intensity of turbulent fluctuations was measured in wind tunnel experiments by Wiggs et al. (1996) and Walker and Nickling (2002b) and may help to explain the maintenance of sediment transport in dune toe region despite an apparent drop in time-averaged velocity and shear stresses.

Downwind of the toe, pressure declines up the windward slope toward a minimum at the crest as streamlines are forced to converge (Fig. 7). This results in a progressive acceleration of flow to a crestal maximum (Fig. 8). The model predicts a near-surface flow acceleration of approximately 40–50% at the crest when compared to upwind velocities that, again, corresponds well with data published by Wiggs et al. (1996) and McKenna Neuman et al. (1997). Unlike some previous attempts at modelling flow over sand dunes (e.g., Weng et al., 1991), the model presented here correctly predicts maximum wind velocities at the crest of the dune itself (as shown in Fig. 8). This is due to the inability of previous models to accommodate the highly turbulent flows in the lee-side separation zone, thereby suppressing the predicted wind velocities at the crest and producing a streamwise velocity maximum upwind of the crest itself.

The accelerated flow up the stoss face of the dune is seen to 'overshoot' the dune brink at the severe break in slope and separates from the surface in the lee (Fig. 8). As noted by Walker and Nickling (2002a) this separated flow creates a region of negative pressure immediately to the lee of the dune as shown in Fig. 7. This results in a low velocity region of reversed flow near the

surface as shown in Fig. 5. This low velocity reversed flow accelerates slightly up the lee-side slip face (Figs. 8 and 9) as noted by Walker and Nickling (2002b). The time-averaged zone of re-attachment at the surface occurs at 9.13 h downwind of the dune crest. This downwind distance is slightly larger than the documented lengths of 4–8 h (Cooke et al., 1993) and 5–10 h suggested by Frank and Kocurek (1996b) and Walker and Nickling (2002c). Sweet and Kocurek (1990) note that the pattern of the lee-side secondary airflow pattern is largely dependent upon the dune geometry and the model presented here provides an excellent opportunity for future testing of the point of re-attachment for dune geometries of markedly differing aspect ratio.

The modelled vertical velocity field (Fig. 9) is similar to experimental findings of Walker and Nickling (2002b). Both studies found positive vertical velocities exist above the stoss slope and over the upper lee slope reflecting the net upward motion caused by topographic forcing and streamline deflection over the stoss and by overshoot and accelerated flows due to separation from the crest respectively. Nevertheless, a difference exists in the location of the region of greatest upward motion. This occurs at the mid-point of the stoss slope in the wind tunnel flow field and close to the dune crest in the model. This disagreement is likely the product of limitations in the wind tunnel flow field, namely the limited sampling grid density of the tunnel experiment with only 3 profiles on the stoss slope (Fig. 1) and limitations of the algorithm used to interpolate the wind tunnel flow field. In both studies, net downward flow occurs beyond the upper lee slope with the zone of greatest downward motion at crestal height 6–12 h downstream of the crest, which is approximately above the flow re-attachment region. This pattern is remarkably similar to that documented over scaled symmetrical fluvial dunes in a recent study by Best and Kostaschuk (2002).

Immediately above the lee-side flow separation region, the model predicts a zone of highly turbulent airflow (TKE up to $5 \text{ m}^2/\text{s}^2$, Fig. 10). This turbulent shear zone in the wake well known in studies of lee-side airflow (e.g., Frank and Kocurek, 1996b; Walker and Nickling, 2002b). The predicted expansion of this turbulent shear zone towards the point of re-attachment followed by dissipation as an internal boundary layer grows downwind of the reattachment point is in correspondence with both field and wind tunnel measurements (e.g., Frank and Kocurek, 1996; Walker and Nickling, 2002b, respectively). Walker and Nickling (2002b) suggest that strong downward velocities in this zone drive flow re-attachment and subsequent boundary layer redevelopment in the lee and propose that the extent of this zone (and consequent flow reattachment distance) is dependent on dune size, form, and spacing. The CFD model will be used to investigate this premise further in additional experiments.

Full recovery of the airflow structure downwind of the point of re-attachment is difficult to define but Fig. 8 suggests that it may occur between 40 and 45 h (limited by the maximum downwind distance of the model calculation domain). Such a distance exceeds the 10–15 h predicted by Lancaster (1989) and is closer to the more recent measurements of 25–30 h by Walker and Nickling (2002c) and corresponds well with the 30–50 h suggested by McLean and Smith (1986) for sub-aqueous dunes.

6. Conclusion

The numerical model presented in this study successfully predicts the flow structure over an idealized transverse dune and validates extremely well to experimental wind tunnel measurements. Moreover, the model seems to correctly simulate the flow in regions of high turbulence and flow reversal, where experimental limitations are unable to provide flow information. Thus, the model provides a complete picture of the flow structure, which is spatially much richer than results produced by current wind tunnel experiments and field studies.

The predicted flow structure has been shown to broadly correspond with current wind tunnel and field data from a range of studies. The flexibility of this model allows testing of a variety of isolated and complex dune morphologies, which are the subjects of forthcoming papers.

Acknowledgements

This work was undertaken whilst Daniel Parsons was in receipt of a NERC studentship GR16/99/FS/2 with additional financial support from the British Geomorphological Research Group (BGRG) to attend the International Conference on Aeolian Research 5. We thank Richard Hardy, Stuart Lane, and members of the BGRG CFD working group for general discussions on numerical modelling. We also thank Nick Lancaster for the research seminar in the Sheffield Geography Department, which was the initial catalyst for this numerical modelling work.

References

- Bates, P.D., Lane, S.N., (Eds.) 1998. High resolution flow modelling. Special issue. *Hydrological Processes* 12, 1129–1396.
- Best, J. L., Kostaschuk, R. A., 2002. An experimental study of turbulent flow over a low-angle dune. *Journal of Geophysical Research, Oceans*, in press.
- Bradbrook, K.F., Biron, P., Lane, S.N., Richards, K.S., Roy, A.G., 1998. Investigation of controls on secondary circulation and mixing

- processes in a simple confluence geometry using a three-dimensional numerical model. *Hydrological Processes* 12, 1371–1396.
- Cooke, R.U., Warren, A., Goudie, A.S., 1993. *Desert Geomorphology*. UCL Press, London.
- Frank, A., Kocurek, G., 1996a. Airflow up the stoss slope of sand dunes: limitations of current understanding. *Geomorphology* 17, 47–54.
- Frank, A., Kocurek, G., 1996b. Toward a model of airflow on the lee side of aeolian dunes. *Sedimentology* 43, 451–458.
- Hodskinson, A., Ferguson, R.I., 1998. Numerical modelling of separated flow in river bends. *Hydrological Processes* 12, 1323–1338.
- Howard, A.D., Moreton, J.B., Gad-el-Hak, M., Pierce, D.B., 1977. Simulation model of erosion and deposition on a barchan dune. NASA Contractor Report CR-2838. NASA: Washington DC.
- Jackson, P.S., Hunt, J.C.R., 1975. Turbulent windflow over a low hill. *Quarterly Journal of the Royal Meteorological Society* 101, 929–955.
- Lancaster, N., 1989. The dynamics of star dunes: an example from the Gran Desierto, Mexico. *Sedimentology* 36, 273–289.
- Lancaster, N., Nickling, W.G., McKenna Neuman, C.K., Wyatt, V.E., 1996. Sediment flux and airflow on the stoss slope of a barchan dune. *Geomorphology* 17, 55–62.
- McKenna Neuman, C., Lancaster, N., Nickling, W.G., 1997. Relations between dune morphology, air flow, and sediment flux on reversing dunes, Silver Peak, Nevada. *Sedimentology* 44, 1103–1113.
- McKenna Neuman, C., Lancaster, N., Nickling, W.G., 2000. The effect of unsteady winds on sediment transport on the stoss slope of a transverse dune, Silver Peak, NV, USA. *Sedimentology* 47, 211–226.
- McLean, S.R., Smith, J.D., 1986. A model for flow over two-dimensional bedforms. *Journal of Hydraulic Engineering* 112, 300–317.
- Mertati, P., Adrian, R.J., 1984. Directional sensitivity of single and multiple sensor probes. *TSI Quarterly* 10, 3–12.
- Nickling, W.G., McKenna Neuman, C., 1999. Recent investigations of airflow and sediment transport over desert dunes. In: Goudie, A.S., Livingstone, I., Stokes, S. (Eds.), *Aeolian Environments, Sediments and Landforms*. John Wiley and Sons, Chichester, pp. 15–47.
- Pantaankar, S.V., Spalding, D.B., 1972. A calculation procedure for heat, mass and momentum transport in three-dimensional parabolic flows. *International Journal of Heat and Mass Transfer* 15, 1782–1799.
- Spalding, D.B., Zhang, Q., 1996. ASAP—Simulating flows with a Cartesian mesh. *Proceedings of the PHOENICS User Conference*, Tokyo, 1996.
- Stam, J.M.T., 1997. On the modelling of two-dimensional aeolian dunes. *Sedimentology* 44, 127–141.
- Sweet, M.L., Kocurek, G., 1990. An empirical model of dune lee-face airflow. *Sedimentology* 37, 1023–1038.
- Versteeg, H.K., Malalasekera, W., 1995. *An Introduction to Computational Fluid Dynamics: the Finite Volume Method*. Longman, London.
- Walker, I.J., 1999. Secondary airflow and sediment transport in the lee of a reversing dune. *Earth Surface Processes and Landforms* 24, 437–488.
- Walker, I.J., Nickling, W.G., 2002a. Dynamics of secondary airflow and sediment transport over and in the lee of transverse dunes. *Progress in Physical Geography* 26, 47–75.
- Walker, I.J., Nickling, W.G., 2002b. Mean flow and turbulence characteristics of simulated airflow over isolated and closely spaced transverse dunes. *Sedimentology*, submitted.
- Walker, I.J., Nickling, W.G., 2002c. Simulation and measurement of surface shear stress over isolated and closely spaced transverse dunes. *Earth Surface Processes and Landforms*, in press.
- Waterson, N.P., 1994. Validation of convection discretisation schemes, VKI Dip Rep. 1994-33, Von Karmen Institute for Fluid Dynamics, Rhode-Saint-Genese, Belgium.
- Weng, W.S., Hunt, J.C.R., Carruthers, D.J., Warren, A., Wiggs, G.F.S., Livingstone, I., Castro, I., 1991. Airflow and sediment transport over sand dunes. *Acta Mechanica* 2 (Supplement), 1–22.
- Wiggs, G.F.S., 1993. Desert dune dynamics and evaluation of wind velocity: an integrated approach. In: Pye, K. (Ed.) *The dynamics and environmental context of aeolian sedimentary systems*. Geological Society Special Publication 72, 37–46.
- Wiggs, G.F.S., 2001. Desert dune processes and dynamics. *Progress in Physical Geography* 25, 53–79.
- Wiggs, G.F.S., Livingstone, I., Warren, A., 1996. The role of streamline curvature in sand dune dynamics: evidence from field and wind tunnel measurements. *Geomorphology* 17, 29–46.
- Wippermann, F.K., Gross, G., 1986. The wind induced shaping and migration of an isolated dune: a numerical experiment. *Boundary-Layer Meteorol* 36, 319–334.
- Wright, C., 1998. Design engineer, TSI Inc., Personal communication.
- Yakhot, V., Orszag, S.A., Thangam, S., Gatshi, T.B., Speziale, C.G., 1992. Development of a turbulence model for shear flow by a double expansion technique. *Physics and Fluids A* 4, 1510–1520.
- Yang, G., Causon, D.M., Ingram, D.M. 1997a. Calculation of 3-D compressible flows around moving bodies. 21st International Symposium on Shock Waves, Australia, July 20–25.
- Yang, G., Causon, D.M., Ingram, D.M., Saunders, R., Batten, P., 1997b. A Cartesian cut-cell method for compressible problems. Part A: static-body problems; part B: moving-body problems. *The Aeronautical Journal of the Royal Aeronautical Society* 101, 47–65.
- Yoon, J.Y., Patel, V.C., 1996. Numerical model of turbulent flow over a sand dune. *Journal of Hydraulic Engineering* 122, 10–18.